RSC Advances

PAPER

View Article Online
View Journal | View Issue

Cite this: *RSC Adv.*, 2024, **14**, 9799

Facile fabrication of a graphene-based chemical sensor with ultrasensitivity for nitrobenzene

Ali Raza,†[a] Zaka Ullah, †*[a] Adnan Khalil,[b] Rashida Batool,[c] Sajjad Haider,[d] Kamran Alam,[e] Nazmina Imrose Sonil,[f] Alvi Muhammad Rouf[f] and Muhammad Faizan Nazar [f]

Received 23rd December 2023
Accepted 8th March 2024

DOI: 10.1039/d3ra08794h

rsc.li/rsc-advances

Chemical sensors have a wide range of applications in a variety of industries, particularly for sensing volatile organic compounds. This work demonstrates the fabrication of a chemical sensor based on graphene deposited on Cu foils using low-pressure chemical vapor deposition, following its transfer on oxidized silicon through a wet etching method. Scanning electron microscopy, Raman spectroscopy and UV-vis spectroscopy of the transferred graphene were performed. A device was fabricated by simply connecting the strips of a Cu tape along the two opposite edges of graphene, which acted as a chemical sensor. The sensor was exposed to different analytes, namely acetone, propanol, benzyl chloride, nitrobenzene, carbon tetrachloride and acetic acid. A relative change in the resistance of the device was observed, which was attributed to the interaction of analytes with graphene as it changes charge concentrations in the graphene lattice. The fabricated sensor showed a notable sensitivity and response time for all analytes, particularly a sensitivity as high as 231.1 for nitrobenzene and a response time as short as 6.9 s for benzyl chloride. The sensor was also tested for analyte leakage from containers for domestic, laboratory and industrial applications.

Introduction

Sensors are devices designed to sense physical variations such as changes in light intensity, temperature, motion, sound, moisture, pressure, and chemicals by converting them into readable electrical signals.[1,2] There is an increasing demand for sensors in a diversity of fields, including automobiles, aerospace, security, environmental monitoring, food industries, manufacturing and pharmaceuticals.[3–5] Graphene consisting of sp^2-hybridized carbon atoms in a hexagonal structure offers high electrical conductivity and ultrathin lattice structure, which endow sensor devices based on graphene with ultrasensitivity and fast response.[6,7] These features make graphene suitable for sensing a wide range of chemicals and gases; however, the sensitivity of a graphene sensor may vary for different analytes. This may also depend on the quality of graphene as it varies significantly, particularly when prepared using different methods such as mechanical exfoliation, epitaxial growth, Hummer's method, or chemical vapor deposition (CVD).[8–10] Researchers have reported various types of chemical sensors with small noise-to-signal ratios for the detection of different chemical species such as acetone, nitrogen dioxide, ammonia, water and carbon monoxide.[8,11,12]

It is important to control the use of products and materials containing volatile organic compounds (VOCs) to protect the environment and human health. VOCs are commonly used in chemical laboratories and industries where their undesired exposures and leakages may result in air pollution, health issues and security concerns.[13,14] Typically, chemical sensors are fabricated using metals and metallic oxides; however, graphene-based sensors have advantages regarding safety, energy consumption and operating conditions such as temperature and humidity. Contrary to this, chemical sensors have some limitations in chemical selectivity and sensitivity for target analytes. A comprehensive review of literature concludes that the preparation of active materials and fabrication of sensors require high-technology equipment and complex processing, which boosts the cost of these sensors.[4,15,16] These are some major problems that are being faced by researchers working in this domain. Therefore, endless efforts are being

[a]*Department of Physics, Division of Science and Technology, University of Education, Lahore 54770, Pakistan. E-mail: zaka.ullah@ue.edu.pk*

[b]*Institute of Physics, Khwaja Fareed University of Engineering and Information Technology, Rahim Yar Khan 64200, Pakistan*

[c]*Department of Chemistry, Division of Science and Technology, University of Education, Lahore 54770, Pakistan*

[d]*Chemical Engineering Department, College of Engineering, King Saud University, PO Box 800, Riyadh 11421, Saudi Arabia*

[e]*Department of Chemical Engineering Materials Environment, Sapienza University of Rome, Rome 00184, Italy*

[f]*State Key Laboratory of Radio Frequency Heterogeneous Integration, College of Electronics and Information Engineering, Shenzhen University, Shenzhen 518060, China*

† These authors contributed equally to this work.

made to assemble chemical sensors that could resolve most of the reported issues.[17–20]

To improve the sensitivity and selectivity of graphene-based chemical sensors, researchers have engineered their outcomes by employing various approaches including controlled synthesis of graphene, integration of nanomaterials with graphene and device designs to offer the efficient response of sensors for a wide range of chemical analytes.[10,11] Here, we report a highly facile and cost-effective strategy to fabricate the graphene-based chemical sensor for VOC analytes. The sensor shows a higher sensitivity and notable response time for a variety of analytes, namely acetone, propanol, benzyl chloride, nitrobenzene, carbon tetrachloride and acetic acid. The sensor offers the highest sensitivity for nitrobenzene and the fastest response for acetone. The studied VOCs are mostly used as solvents in the preparation of several other compounds/materials including antifreeze, lacquer, soap and dyes. The demonstrated sensor can be used to detect the presence and leakage of VOCs in industries and places where these are prepared. The use of fabricated sensors may save extensive losses during leakage detection and may anticipate serious damages and destructions in time to avoid alarming irreparable losses.

Experimental

The deposition of graphene films on copper foils using low pressure chemical vapor deposition (LPCVD) was achieved following the procedure reported in the reported literature.[9] The deposited graphene was transferred on a silicon wafer using the wet etching method. Scanning electron microscopy (Quanta 400 FEG, USA), Raman spectrometry (LabRam HR800-UV-NIR, USA, λ = 532.15 nm) and UV-visible spectrometry (Agilent 630) were employed for inspecting the morphological, quality and optical features of graphene films, respectively. Moreover, X-ray diffractometry (German, D8 Advance) and X-ray photoelectron spectrometry (ULVAC-PHI 5000 Versaprobe II) were used to inspect the structural and chemical states of the graphene films, respectively.

Device fabrication

For device fabrication, thin (~3 mm wide) strips of copper tapes were attached along the two opposite edges of the films, which were then connected with the Keithley sourcemeter 2400 during the testing of the sensor. The surface of the sensor was exposed to analytes and the response of the sensor was recorded for acetone, propanol, benzyl chloride, nitrobenzene, carbon tetrachloride and acetic acid.

Results and discussion

Fig. 1(a) depicts the route for the sample preparation and device fabrication. Graphene was deposited on Cu foils using LPCVD and transferred onto silicon wafers through the wet etching method. Cu tape strips were attached to graphene along the two opposite edges. Fig. 1(b) shows the Raman spectrum of graphene, which indicates the quality and layer count of graphene. Characteristic D (caused by transverse optical phonons near the *K* point), G (due to optical E2g phonons at the centre of the Brillouin zone), and 2D (attributed to the two types of phonons with opposite momenta) peaks were observed around 1347, 1581 and 2699 cm^{-1}, respectively, which evidence the presence of the sp^2-bonded carbon atoms forming the graphene layer. It was found to be a multilayer (~5 layers). To further estimate the graphene quality, the defect density (n_{do}) was measured using the following formula:[9]

$$n_{do} = \left[\frac{1}{L_\alpha}\right]^2$$

where, L_α is the grain size, which was calculated as:[21]

$$L_\alpha = \left[2.4 \times 10^{-10}\ \text{nm}^{-3}\right] \lambda_L{}^4 \left[\frac{I_D}{I_G}\right]^{-1}$$

Here, λ_L is the excitation laser wavelength, which was 532.15 nm; the intensities I_D and I_G of D and G peaks, respectively, were calculated from the Raman spectrum; the value of the grain size (L_α) was calculated as 60.91 nm and that of the defect density (n_{do}) as 2.69×10^{10} cm^{-2}. These results ensure that the graphene quality was sufficiently high for the fabrication of the electronic devices. Fig. 1(c) shows the transmittance spectrum of graphene which gives ~88% transmittance at 550 nm wavelength for five-layer graphene. As monolayer graphene is about 97.7% transparent for the visible spectrum, the optical spectrum also suggests that the deposited graphene was five layers thick.[9] To further examine the quality of graphene and its suitability for the fabrication of transparent electronic devices, the optical and dc conductivities, which depend upon the transmission (T) and sheet resistance (R_s), were calculated using the following relation:[9]

$$T = \left(1 + \frac{Z_o}{2R_s}\frac{\sigma_{op}}{\sigma_{dc}}\right)^{-2}$$

Here, σ_{op} is the optical conductivity, σ_{dc} is the dc conductivity, and Z_o is the impedance of free space with a value of 377 Ω. The conductivity ratio (σ_{dc}/σ_{op}) was found to be 0.966 for the deposited graphene. The inset images in Fig. 1(b) and (c) show the SEM micrographs of the deposited graphene, which evidenced the sufficient uniformity of graphene for the fabrication of the electronic devices.

Fig. 1(d) displays the X-ray diffraction (XRD) pattern of the LPCVD-deposited multilayer graphene. Typically, the graphene layer being single-atom thick did not show any obvious diffraction peak. However, as the number of graphene layers is increased, a peak around 2θ as 26° appears in the pattern. The peak becomes sharper with the increase in graphene layers and gets prominent for graphite (graphene stack with more than 8 layers). In the current scenario, a hump appears at the 2θ value of 26.1°, which is indexed as 002 as per JCPDS card no. 75-1621. The observation is consistent with the reported data.[22] Fig. 1(e) shows the X-ray photoelectron spectroscopy (XPS) response of the multi-layer graphene. The typical peak observed at 284.06 eV is attributed to the C–C bond. The peak is fitted using the Gaussian utility. It further suggests the presence of graphitic sp^2 carbon which actually forms the graphene layers. The response is consistent with already reported results in the literature.[23,24]

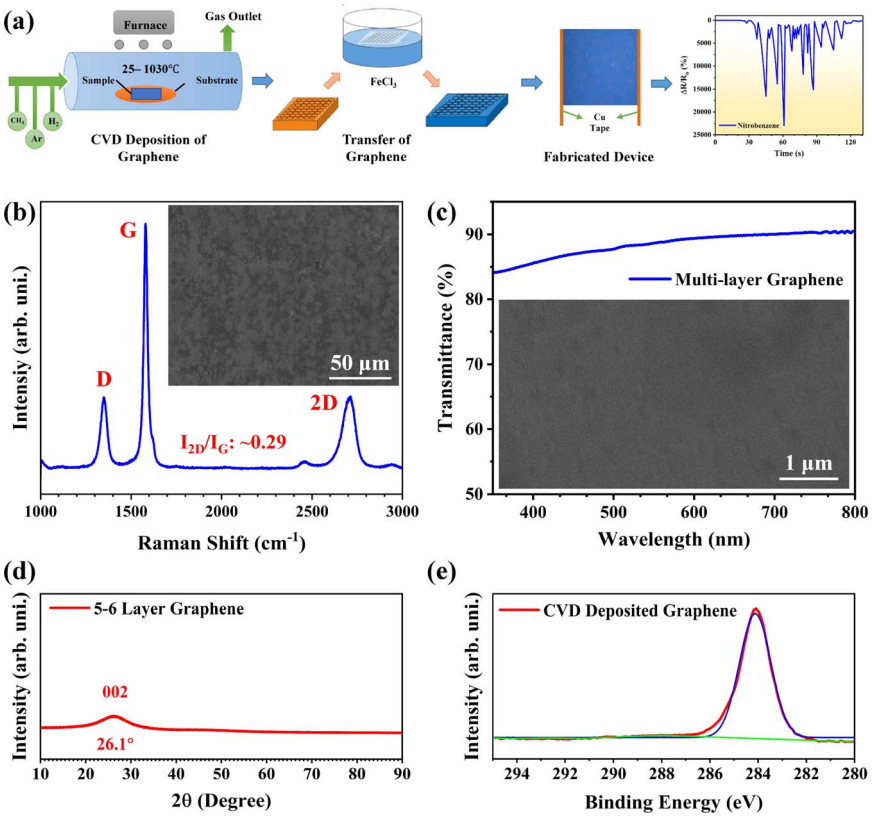

Fig. 1 (a) Schematic illustration showing the route of the performed work. (b) Raman spectroscopy and (c) UV-visible spectroscopy of multi-layer graphene. Insets in (b) and (c) show the low and high-resolution SEM images, respectively. (d) XRD and (e) XPS spectra of CVD deposited graphene.

Fig. 2 depicts the response of the graphene sensor when different analytes are exposed to the sensor in the form of small droplets at room temperature. As these analytes come in contact with the active material (graphene), these are physically adsorbed on the surface of the graphene and change its concentration of charge carriers which ultimately changes the resistance of graphene.[20] It can be noticed that initially for around 20 s, the resistance of the sensor did not show any obvious changes for all the analytes as these have not been exposed to the sensor. However, upon exposure to the analyte, the resistance of the sensor started to increase. It is notable that the relative change in the resistance is not uniform, instead, it fluctuates between minimum to maximum values. The mechanism of quick response and recovery of the sensor can be associated with the non-destructive 2D structure of graphene, which facilitates the mass transfer of the analyte molecules in the form of electron transfer to and from the region of interaction. Generally, analytes behave as an accepter and electrons flow from the graphene to the analyte making the graphene a p-type doped layer. Fortunately, graphene promotes the adsorption of analyte molecules on its surface.[22,25] Due to this abrupt transfer of charges to and from the analyte, continuous fluctuations were observed for a long time and the value of relative resistance was increased by approximately 8701, 5419, 12, 23 112, 325 and 17 391% for acetone, propanol, benzyl chloride, nitrobenzene, carbon tetrachloride and acetic acid, respectively. Moreover, resistance fluctuations of the sensor are attributed to uneven exposure of the analyte. It is also important to mention that as the analyte molecules are exposed to the sensor surface, these start to evaporate. After a specific time (~90 s) most of the analyte gets evaporated and the resistance of the sensor is almost restored, as shown in Fig. 2. The resistance restoration time, 15.6 to 61.2 s for all analytes considered in this study, depends upon volatility, concentration and interaction tendency of the analytes.[26] The sensing mechanism of the demonstrated sensor is illustrated in Fig. 3.

The sensitivity and response time of a chemical sensor are the two fundamental criteria to evaluate its performance. The sensitivity of the demonstrated graphene sensor was determined using the typical relation, $S = (R_a - R_o)/R_o$, where S is the sensitivity, R_a is the resistance of the sensor upon exposure to the analyte, and R_o is the resistance of the sensor before the exposure of the analyte.[27] The sensitivity of the sensor was recorded as 1.1, 4.3, 55.2, 88.1, 174.9 and 231.1 for benzyl chloride, carbon tetrachloride, propanol, acetone, acetic acid and nitrobenzene, respectively, as shown in Fig. 4. Whereas, the response time of the sensor was measured as 6.9, 11.2, 27.9, 51.5, 31.3 and 24.8 s for benzyl chloride, carbon tetrachloride, propanol, acetone, acetic acid and nitrobenzene, respectively. Moreover, the recovery time of the graphene sensor was found as 58.7 (~50%), 33.1 (~92%), 15.6 (~99%), 16.4 (~99%), 42.4 (~80%) and 61.2 s (~100%) for benzyl chloride, carbon

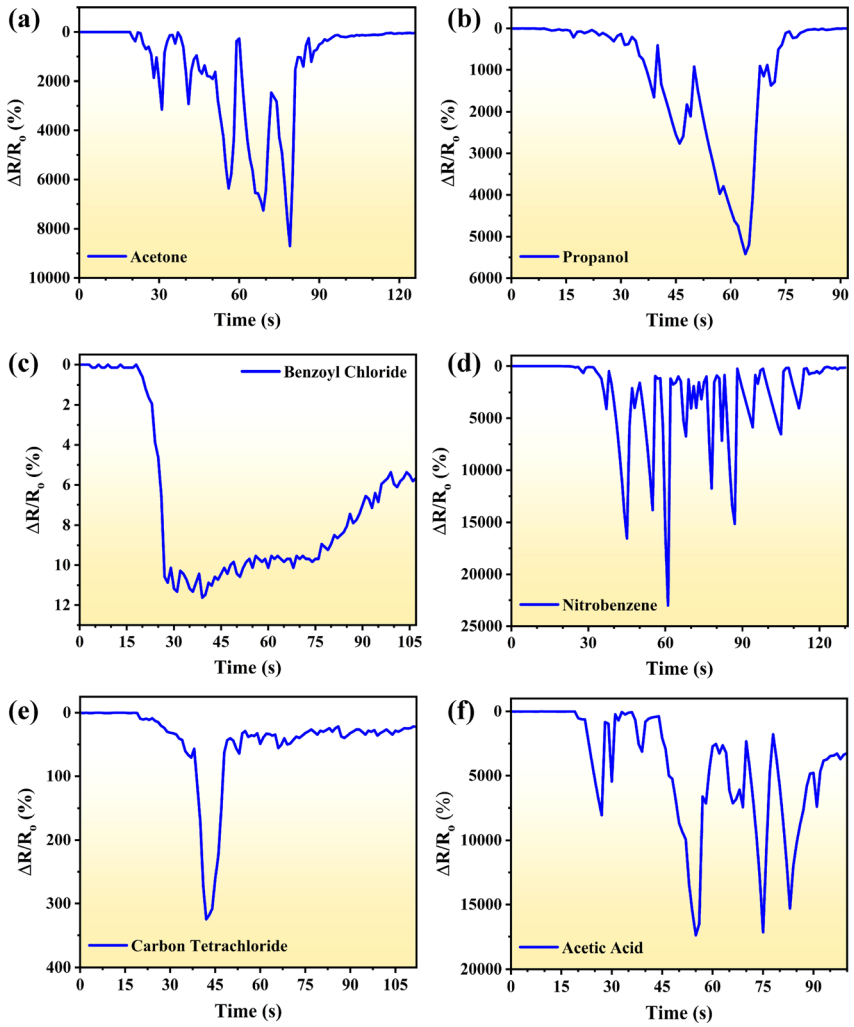

Fig. 2 Real time response of the graphene sensor for (a) acetone, (b) propanol, (c) benzoyl chloride, (d) nitrobenzene, (e) carbon tetrachloride and (f) acetic acid.

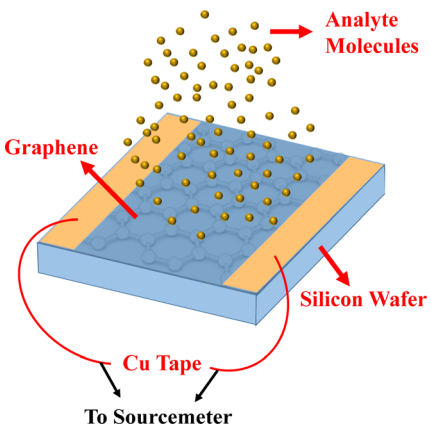

Fig. 3 Schematic illustration depicting the sensing mechanism of the graphene sensor.

tetrachloride, propanol, acetone, acetic acid and nitrobenzene, respectively. It is worth mentioning that the sensor not only offers the highest sensitivity and notable response time for nitrobenzene but also shows almost 100% recovery in a short time, which enables its reusability for the desired applications. Table 1 shows the comparative analysis of the performance of the demonstrated sensor with that reported in the literature for the investigated analytes.

In order to investigate if the demonstrated sensor responds to any exposed chemical or if it has some satisfactory selectivity, it was made to interact with a blank solution (deionized water). The relative change in resistance of the sensor ($\Delta R/R_o$, %) was neglectable (well below 5%). Consequently, it was evidenced that the sensor did not respond to all the chemicals. Moreover, Fig. 4 shows that the minimum response of the sensor was offered to benzoyl chloride, which was even ~510%. When it is compared with the response to the blank solution, the aforementioned outcome was further supported. Furthermore, the deeper analysis of the results given in Fig. 4 ensured the notable selectivity of the demonstrated sensor. The minimum difference in the response of the sensor for any two tested analytes is between 610 and 12990%, which is highly sufficient, and may enable not only to sense the chemical but also to identify it accurately.

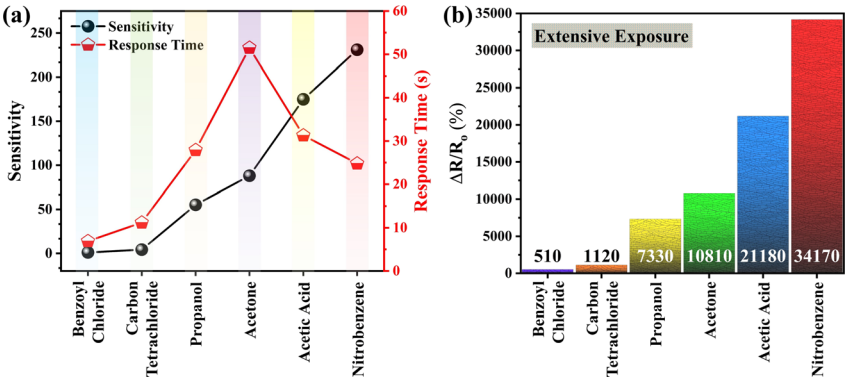

Fig. 4 (a) Sensitivity and response time of the demonstrated sensor. (b) Response of the sensor upon extensive exposure to all the considered analytes for a longer time.

Table 1 A comparison of the performance of the demonstrated sensor with other sensors reported in the literature for the studied analytes

Sensing material	Analyte	Response time (s)	Sensitivity	Ref.
PVA/CuO	Propanol	342.0	73	13
PVA/CuO/Gr-NPIs	Propanol	366.0	73	13
Graphene	Propanol	27.9	55	This work
MGO/$G_{0.1}$	Acetic acid	50.0	363	28
GQDs-ZnO	Acetic acid	43.0	—	29
$Zn_{0.96}Mg_{0.04}O$	Acetic acid	145.0	136%	30
Graphene	Acetic acid	31.3	175	This work
ZIF-8@ZnO/$TiO_{2.1}$DTDPC	CCl_4	0.3	0.05 nm ppm^{-1}	31
Graphene	CCl_4	11.2	4	This work
PAA-AgNPs/GC	Nitrobenzene	—	7.88 μA μM^{-1}	32
EAG/SPCE	Nitrobenzene	5.0	1.445 μA μM^{-1} cm^{-2}	33
PCN-224-QCM	Nitrobenzene	16.0	—	34
Graphene	Nitrobenzene	24.8	231	This work
TiO_2/Co_3O_4	Acetone	122.0	—	35
$AuSnO_{2-2}$	Acetone	18.2	—	36
Graphene	Acetone	51.5	88	This work
Graphene	Benzoyl chloride	6.9	1	This work

All the studied analytes/compounds are volatile and offer a diversity of industrial applications. Particularly, these are used at large scale in industries for the preparation of a variety of materials including plastics, dyes, insecticides, photographic chemicals, rubbers, inks, textiles, medical products, printing materials, skin products, cleaning gadgets and solvents for organic compounds. Special precautions are required at all times for their handling and storage, as their external exposure or leakage may lead to drastic losses. To avoid such losses, the demonstrated graphene sensor may act as a leakage sensor for these analytes/volatile organic compounds. Such suitability allows the sensor to be brought in continuous exposure to these analytes and to record their response. Fig. 4(b) shows the response of the sensor with maximum change in its relative resistance that is sufficient for leakage applications. The sensor can inform about the leakage of these chemicals particularly during their preparation, transportation, storage and usage. For a prototype fabrication of this sensor, an alarm can be attached to the device which may ring upon the change in the resistance of the sensor up to a specific range, caused by the exposure of the analyte in the given scenarios. Consequently, the sensor may be successfully employed for the timely detection of leakage of these chemicals in a variety of industries. Moreover, for typical practical applications, these can be acquired for environmental monitoring, agriculture purposes, food protection, public safety, disease detection and military security.[4,5,15]

Conclusions

In summary, graphene was deposited on Cu foils using LPCVD, transferred on oxidized silicon and characterized using SEM, Raman spectroscopy, UV-visible spectroscopy, XRD and XPS. The results confirmed the deposition of five-layer graphene with a defect density of 2.69×10^{-10} cm^{-2} and transparency of ~88% for 550 nm. The graphene was used for the fabrication of chemical sensors through a facile approach, and it was tested for six different analytes. The sensor delivered a remarkable sensitivity and response time for acetone, nitrobenzene and acetic acid. The highest sensitivity was recorded as 231.1 for nitrobenzene, and the fastest response with a response time of

6.9 s for benzoyl chloride. The sensor was also tested for extensive leakage of these chemicals and it offers valuable leakage detection performance. The demonstrated sensor can be useful for sensing the studied VOCs in different industries including plastic, dyes, insecticide, photographic chemicals, rubber, printing, textile, medical, skin, paint and ink.

Author contributions

Ali Raza: conceptualization, methodology, software, investigation, writing – original draft. Zaka Ullah: conceptualization, methodology, software, validation, investigation, writing – original draft. Adnan Khalil: software, validation, formal analysis. Rashida Batool: software, validation. Sajjad Haider: resources, funding acquisition. Kamran Alam: resources, funding acquisition. Nazmina Imrose Sonil: validation, writing – review and editing. Alvi Muhammad Rouf: software, writing – review and editing, visualization. Muhammad Faizan Nazar: resources, supervision, project administration, funding acquisition.

Conflicts of interest

There are no conflicts to declare.

Acknowledgements

The authors sincerely appreciate the funding from Researchers Supporting Project number RSP2024R399, King Saud University, Riyadh, Saudi Arabia.

Notes and references

1 X. Yu, L. Fu, T. Wang, Z. Liu, N. Niu and L. Chen, *Chin. Chem. Lett.*, 2023, 109167, DOI: 10.1016/j.cclet.2023.109167.
2 K. Muthumalai, N. Gokila, Y. Haldorai and R. T. Rajendra Kumar, *Adv. Sens. Res.*, 2023, 2300107.
3 X. Xu, J. Zhou, Y. Xin, G. Lubineau, Q. Ma and L. Jiang, *Sci. Rep.*, 2017, **7**, 4317.
4 W. Li, Z. Zhu, Q. Chen, J. Li and M. Tu, *Cell Rep. Phys. Sci.*, 2023, 101679, DOI: 10.1016/j.xcrp.2023.101679.
5 T. A. Saleh and G. Fadillah, *Trends Environ. Anal. Chem.*, 2023, **39**, e00204.
6 M. Aliofkhazraei, *Advances in Graphene Science*, BoD – Books on Demand, 2013.
7 Z. Ullah, Q. Li, R. Wang, Q. Zeng, W. Li and L. Liu, *IEEE Trans. Nanotechnol.*, 2018, **17**, 65–68.
8 W. Li, X. Geng, Y. Guo, J. Rong, Y. Gong, L. Wu, X. Zhang, P. Li, J. Xu and G. Cheng, *ACS Nano*, 2011, **5**, 6955–6961.
9 Z. Ullah, S. Riaz, Q. Li, S. Atiq, M. Saleem, M. Azhar, S. Naseem and L. Liu, *Mater. Res. Express*, 2018, **5**, 035606.
10 F. Yavari and N. Koratkar, *J. Phys. Chem. Lett.*, 2012, **3**, 1746–1753.
11 A. R. Jang, J. E. Lim, S. Jang, M. H. Kang, G. Lee, H. Chang, E. Kim, J. K. Park and J.-O. Lee, *Appl. Surf. Sci.*, 2021, **562**, 150201.
12 A. M. Pasqualeti, F. M. Shimizu, L. P. de Oliveira, R. A. G. de Oliveira, R. M. de Carvalho, R. A. Fontes, A. L. Gobbi and R. S. Lima, *TrAC, Trends Anal. Chem.*, 2023, **168**, 117305.
13 G. J. Thangamani, K. Deshmukh, K. Chidambaram, M. B. Ahamed, K. K. Sadasivuni, D. Ponnamma, M. Faisal, N. A. Nambiraj and S. K. K. Pasha, *J. Mater. Sci.: Mater. Electron.*, 2018, **29**, 5186–5205.
14 V. Galstyan, A. Moumen, G. W. C. Kumarage and E. Comini, *Sens. Actuators, B*, 2022, **357**, 131466.
15 N. Promphet, S. Ummartyotin, W. Ngeontae, P. Puthongkham and N. Rodthongkum, *Anal. Chim. Acta*, 2021, **1179**, 338643.
16 J. Brunet, L. Spinelle, A. Ndiaye, M. Dubois, G. Monier, C. Varenne, A. Pauly, B. Lauron, K. Guerin and A. Hamwi, *Thin Solid Films*, 2011, **520**, 971–977.
17 M. Wusiman and F. Taghipour, *Water Res.*, 2024, **249**, 120972.
18 R. Schneider, M. H. M. Facure, K. B. R. Teodoro, L. A. Mercante and D. S. Correa, *ACS Appl. Nano Mater.*, 2023, **6**, 22435–22445.
19 S. Kim, T. Y. Ko, A. K. Jena, A. S. Nissimagoudar, J. Lee, S. Lee, T. Oh, Y. C. Kang, I. In, S. Bhattacharjee, C. M. Koo, S.-C. Lee and S. J. Kim, *Adv. Funct. Mater.*, 2023, 2310641.
20 Z. Ullah, A. Rehman, B. Rehman, M. Altaf, N. I. Sonil, S. Atiq, M. Saleem, M. Azhar, S. Riaz and S. Naseem, *Microelectron. Eng.*, 2021, **250**, 111638.
21 J. Hu, J. Xu, Y. Zhao, L. Shi, Q. Li, F. Liu, Z. Ullah, W. Li, Y. Guo and L. Liu, *Sci. Rep.*, 2017, **7**, 45358.
22 S. Srivastava, K. Jain, V. N. Singh, S. Singh, N. Vijayan, N. Dilawar, G. Gupta and T. D. Senguttuvan, *Nanotechnology*, 2012, **23**, 205501.
23 M. Z. Iqbal, M. W. Iqbal, M. F. Khan and J. Eom, *Phys. Chem. Chem. Phys.*, 2015, **17**, 20551–20556.
24 S. Hussain, M. W. Iqbal, J. Park, M. Ahmad, J. Singh, J. Eom and J. Jung, *Nanoscale Res. Lett.*, 2014, **9**, 546.
25 C. Yang, T. Chen, Y. Yang, M. Hsiao, M. Meyyappan and C. Lai, *Vacuum*, 2017, **140**, 89–95.
26 C.-M. Yang, T.-C. Chen, Y.-C. Yang, M.-C. Hsiao, M. Meyyappan and C.-S. Lai, *Vacuum*, 2017, **140**, 89–95.
27 S. Goutham, K. K. Sadasivuni, D. S. Kumar and K. V. Rao, *RSC Adv.*, 2018, **8**, 3243–3249.
28 L. He, C. Gao, L. Yang, K. Zhang, X. Chu, S. Liang and D. Zeng, *Sens. Actuators, B*, 2020, **306**, 127453.
29 X. Chu, P. Dai, Y. Dong, W. Sun, L. Bai and W. Zhang, *J. Mater. Sci.: Mater. Electron.*, 2017, **28**, 19164–19173.
30 V. Khorramshahi, J. Karamdel and R. Yousefi, *J. Mater. Sci.: Mater. Electron.*, 2018, **29**, 14679–14688.
31 K. Zhan, Y. Xing, Y. Zhu, J. Yan and Y. Chen, *Sens. Actuators, A*, 2020, **314**, 112249.
32 V. M. Kariuki, S. A. Fasih-Ahmad, F. J. Osonga and O. A. Sadik, *Analyst*, 2016, **141**, 2259–2269.
33 B. Thirumalraj, S. Palanisamy and S.-M. Chen, *Int. J. Electrochem. Sci.*, 2015, **10**, 4173–4182.
34 L. Wang, J. Song, Y. Wu and C. Yu, *J. Porous Mater.*, 2023, **30**, 1617–1623.
35 Z. Cai and S. Park, *J. Alloys Compd.*, 2022, **919**, 165875.
36 L. Guo, Z. Shen, C. Ma, C. Ma, J. Wang and T. Yuan, *J. Alloys Compd.*, 2022, **906**, 164375.